ARCHIVES OF ELECTRICAL ENGINEERING VOL. 66(4), pp. 705-715 (2017)

DOI 10.1515/aee-2017-0053

Heat generation by eddy currents in a shell of superconducting bus-bars for SIS100 particle accelerator at FAIR

ŁUKASZ TOMKÓW[1], STANISŁAW TROJANOWSKI[2], MARIAN CISZEK[1, 2], MACIEJ CHOROWSKI[1]

[1]*Faculty of Mechanical and Power Engineering, Wrocław University of Technology*
Wybrzeże St. Wyspiańskiego 27, 50-370 Wrocław, Poland

[2]*Institute of Low Temperature and Structure Research*
Okólna 2, 50-422 Wrocław
e-mail: lukasz.tomkow@pwr.edu.pl

(Received: 02.03.2017, revised: 12.08.2017)

Abstract: Superconducting magnets in the SIS100 particle accelerator require the supply of liquid helium and electric current. Both are transported with by-pass lines designed at Wrocław University of Technology. Bus-bars used to transfer an electric current between the sections of the accelerator will be encased in a steel shell. Eddy currents are expected to appear in the shell during fast-ramp operation of magnets. Heat generation, which should be limited in any cryogenic system, will appear in the shell. In this work the amount of heat generated is assessed depending on the geometry of an assembly of the bus-bars and the shell. Numerical and analytical calculations are described. It was found that heat generation in the shell is relatively small when compared to other sources present in the accelerator and its value strongly depends on the geometry of the shell. The distribution of eddy currents and generated heat for different geometrical options are presented. Based on the results of the calculations the optimal design is proposed.

Key words: superconductors, eddy currents, electromagnetic heat generation, particle accelerators

1. Introduction

Modern particle accelerators require high magnetic fields to bend and shape particle beams. Therefore they need to be reliably supplied with large electrical currents. Power for the SIS100 accelerator, currently under construction at GSI, Darmstadt, Germany, is going to be transmitted by superconducting bus-bars [1]. The bus-bars together with helium transfer lines form by-pass lines. They are the part of Polish in-kind contribution to the FAIR project. The

effort is coordinated by Jagiellonian University of Krakow. Bypass lines are designed, manufactured and commissioned by Wrocław University of Technology [2]. In the bus-bars Nuclotron-type cables will be used, with NbTi serving as a material for superconducting filaments [3, 4]. Critical temperature of this material at zero magnetic field is approximately 9.2 K and it is going to be cooled with forced two-phase liquid helium flow. High temperature superconductors also are going to be applied at SIS100, as the part of current leads [5].

Due to large cooling power requirements and the risk of quench, the margin of the heat budget of the entire accelerator and its subsystems is extremely low. For example, the expected heat load of Super-FRS (separating device) is 1770 W at 4 K, including a design factor of 1.5 [6]. Cooling capacity of the entire cryogenic system of accelerator is approximately 34.9 kW at 4 K [7]. Given that, any heat generation that might appear should be assessed, quantified and limited. Additional heat loads must be removed, thus more cooling power is needed. It can also be dangerous due to the increased risk of quench. Additional challenge is the fact that an electric current and liquid helium will be transported in a single assembly.

SIS100 magnets are going to operate under several regimes [8]. AC losses occurring in superconducting magnets were calculated analytically [9] and measured experimentally [10, 11]. They were found to be major heat input for both SIS100 [12] and its planned extension, SIS300 [13]. Magnet design was significantly affected by thermal issues [14]. A proper cooling system will be introduced [15].

Bus-bars will be the part of a by-pass line. Some sources of heat are expected to be present there. The first is a bus-bar itself, with AC losses occurring [16]. Eddy currents induced in non-superconducting parts of the accelerator by fast-ramping currents in magnets and bus-bars are the additional sources of heat. Eddy currents power in the support structure of the magnet was calculated previously and was found to be relatively high, when compared to heat budget [17].

In by-pass lines analysed in this paper the pairs of bus-bar lines will be encased in a steel tube to provide thermal and electrical shielding [18]. This work presents the results of analytical and numerical results of the calculation of heat generation by eddy currents occurring in a shell of bus-bars. The major goal of this work was to assess the heat generation and to find the optimal shape of the bus-bars and shell assembly, which would lead to the minimisation of heat generation. In the future by-pass lines will be tested experimentally along with the superconducting magnets [19].

2. Methods

2.1. General assumptions

Bus-bar assembly contains two superconducting Nuclotron-type cables surrounded by a steel shell. The cables are cooled by liquid helium flowing in a pipe around which a superconductor is wound. The cross-section of the line with dimensions marked is shown in Figure 1. R denotes the internal radius of the shell which, in the case of considered line, is equal to 14 mm. ΔR is the thickness of the shell equal to 1 mm, r is the external radius of

a superconducting cable equal to 3.75 mm, r' is the internal radius of the cable, assumed as 2.6 mm.

The effect of variation of some geometric parameters on the size of heat generation was considered during the calculations. The first parameter is ζ, defined with Equation (1).

$$\zeta = \frac{\xi}{R} . \tag{1}$$

ξ is here the distance between the axes of the shell and the cable. The shell can be either solid or split along its length in two halves. Numerical calculations are performed for both solid and split shell, while analytical only for a solid shell. In the case of split shell an additional varied parameter was β – the angle between the split and a line connecting axes of the cables.

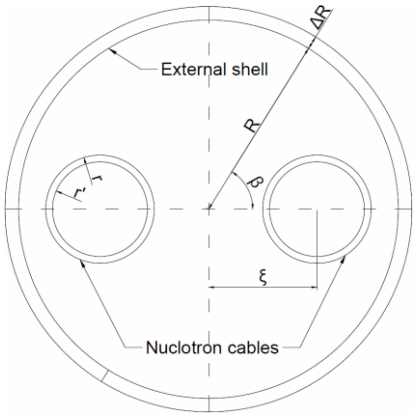

Fig. 1. Geometrical dimensions of the considered line

The accelerator will be supplied with power in several different modes. The highest heat generation in the shell is expected during the operation under a fast-ramp regime. In this regime the current is going to be varied between 0 and 14 kA in triangular cycles, which are going to be executed with a frequency of 1 Hz [8], giving a local increase speed of the current of approximately 28~kA/s. Electrical conductivity σ of the shell is assumed to be constant and equal to $1.54 \cdot 10^6$ S/m at a temperature of 300 K. At an operation temperature of 4 K it is expected to be approximately 30% higher [20]. 2D and 3D numerical models of a bus-bar and shell assembly were created and an analytical solution for solid shell was used to validate them.

2.2. Analytical

The section of the solid shell with uniform conditions is considered. Effects appearing at the ends of the shell and non-straight sections are therefore neglected. Local volumetric power density of eddy currents *dP* is calculated using Formula (2).

$$dP = \frac{j^2 dV}{\sigma}, \tag{2}$$

where j is the local density of eddy currents, V is the volume. In order to obtain total energy dissipation integration should be performed over angular direction θ, length l and in the radial direction. Several simplifications can be applied. Variation in radial direction can be assessed based on skin depth δ. Applying Fourier series expansion to the triangular function yields only odd non-zero harmonics, with amplitude decreasing with the square of their number. The amplitude of the ninth harmonic is only 1.2% of the amplitude of the first harmonic. Skin depth is calculated with Equation (3).

$$\delta = \sqrt{\frac{2}{\sigma\omega\mu_0}}, \tag{3}$$

where ω is the pulsation of a given harmonic, μ_0 is the magnetic permeability of vacuum. Skin depth for the ninth harmonic is approximately 135 mm. For a base harmonic of 1 Hz it is more than 405 mm. Skin depth at the given power regime is much larger than the thickness of the shell and neglecting radial variation of current density will lead to errors of less than 1%. Since uniform conditions over the length of the shell are assumed this term can also be neglected. l is assumed as 1~m to obtain the value of heat generation per meter length. Therefore, only integration over θ is needed, yielding Formula (4).

$$P = \frac{R\Delta R l \int_0^{2\pi} j^2(\theta)\mathrm{d}\theta}{\sigma}. \tag{4}$$

Angular distribution of eddy current density has to be found. Since the rate of change of the current in the bus-bars is linear for the majority of the time it can be assumed that the rate of change is constant and the distribution of currents does not change in time. The current has only component in direction l, therefore it is sufficient to calculate the derivative of magnetic flux through a shell wall over time t in the region symmetrical with respect to the line of zero current. The value of electric field E at the edges of the integration region is found applying Faraday's law (Formula (5)).

$$E = -\frac{\mathrm{d}\phi}{\mathrm{d}t}\frac{1}{2l}. \tag{5}$$

Eddy current density is calculated using Ohm's law (6), thus giving all parameters needed in Formula (4).

$$j = \sigma E. \tag{6}$$

2.3. Numerical models

Numerical models of the considered system were developed using the AC/DC package of commercial software Comsol. The base equation for the model is Ampère's law. Initially a 2D

model of the transfer line with a solid shell was created and validated against the analytical solution. A 3D model of a transfer line with the solid shell was created. After the validation of this model the dependence of heat generation on β was calculated for a half of the shell.

In the 2D model the entire geometry was recreated, including the shape of bus-bars. In the case of the analytical calculations only point currents were assumed, while in the 3D models linear currents were applied. In the 2D model the bus-bars were modelled as uniformly distributed current density. In the actual system some variation in current density distribution will appear due to the properties exhibited by superconducting material, especially flux pinning. However, these variations appear only locally and do not significantly affect the distribution of a magnetic field at some distance from the cable. They were not modelled in order for computational power to be saved.

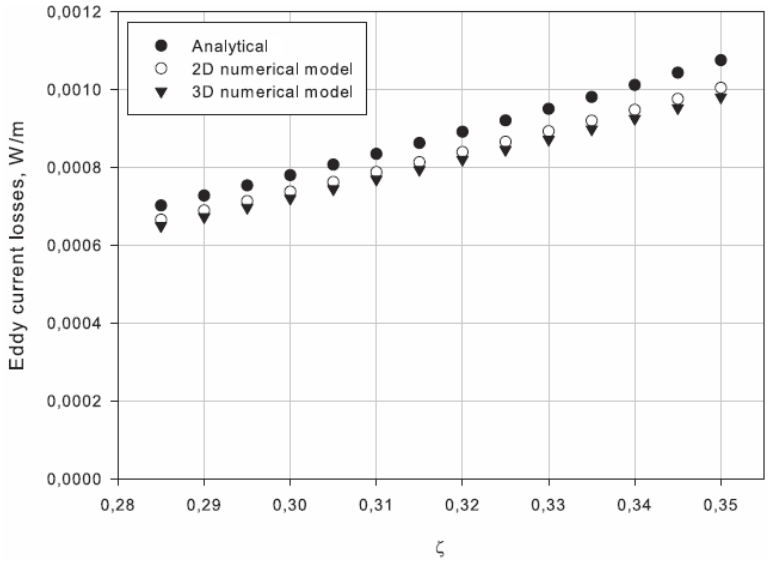

Fig. 2. Comparison of heat generated by the dissipation of eddy currents in W/m in dependence on parameter ζ in the full shell calculated analytically and with numerical models

For every model the region between bus-bars and the shell was assumed to be vacuum with a relative permeability and permittivity of 1. Electrical conductivity of this region is assumed to be 10 orders of magnitude lower than of the shell. The current in the bus-bars is assumed to be linearly increasing with a speed of 28 kA/s. In both bus-bars the current is flowing in different directions. In the 3D models the sections with a length of 200 mm were modelled. The distribution of currents and heat generation density in the middle cross-section of the shell was analysed to reduce the effect of variations at the ends of the modelled region.

The models were validated against each other and an analytical solution. The variation of total heat generation depending on parameter ζ was analysed for both solid and split shells. For the split shell additionally the dependence on the angle of split location β was found. The models also yield the distribution of eddy currents and a magnetic field.

3. Results

The most important results have been shown graphically in the following figures. Integration of heat generation by eddy current over the surface of a cross-section yields the value of heat generation per meter length of the transfer line. The results obtained from numerical models and analytical calculations are compared in Figure 2 in order for their reliability to be assessed.

Figure 3 shows the example of results of numerical calculations for the full shell performed with the 2D numerical model for the parameter ζ of 0.35. Distribution of eddy currents density and resulting heat dissipation are presented. The horizontal line in this figure and in Figure 4 marks the line connecting the axes of bus-bars.

Figure 4 shows the changes in distribution of eddy currents and resistive heat generation in the cross-section of half of a split shell depending on angle β. The cables are placed horizontally. Parameter ζ used during the calculations for the figures was equal to 0.35.

The application of a 3D model allowed to find the shape of eddy currents for different geometries. Figure 5 shows the comparison between streamlines of eddy currents for both a full shell and split shell. Several angles have been analysed. In the cases when the shell is split, only half of the shell is shown for greater clarity.

Figure 6 shows the dependence of eddy current heat generation in a split shell on geometrical parameters. Heat generation was calculated in a single half of shell for the pairs of β and ζ and integrated over the central cross-section.

4. Discussion

The obtained results appear to be reliable. The comparison between the results obtained from 2D and 3D numerical models of a full shell shows that the differences are almost negligible. Possible discrepancy can come from lower mesh density of the 3D model or the effects appearing at the ends. It can be seen in Figure 2 that the heat generation calculated with numerical models is slightly lower than the one obtained analytically. It is caused by the simplifications assumed during the analytical calculations, especially the lack of analysis of radial current distribution. In the face of small difference between the 2D and 3D model the effect of assumption of point currents seems to be negligible.

Distribution of eddy currents at the full shell, shown in Figures 3 and 4, is symmetric with respect to two axes – the line connecting two axes of bus-bars and perpendicular one intersecting at the axis of the shell. Eddy currents flow in two loops. The maximum current density and heat generation appear in the region close to the intersection of the line connecting the axes of bus-bars and walls of the shell. In the case of horizontal bus-bars arrangement zero current appears directly above and below the axis of the shell. In this region heat generation is the lowest.

Changes to both the distribution and size of currents can appear when the shell is divided in two and depend on the angular position of split defined by angle β. When the shell is

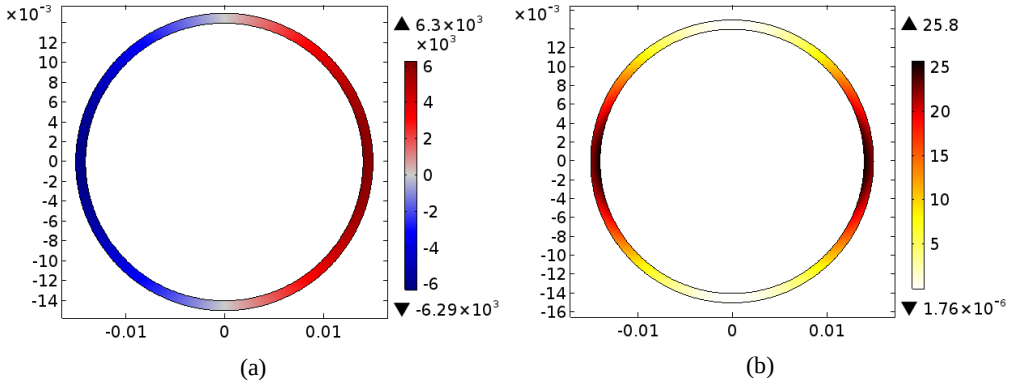

Fig. 3. Distribution of eddy currents density j in A/m^2: (a) and heat generation caused by them in W/m^3; (b) shown on the cross-section of the shell

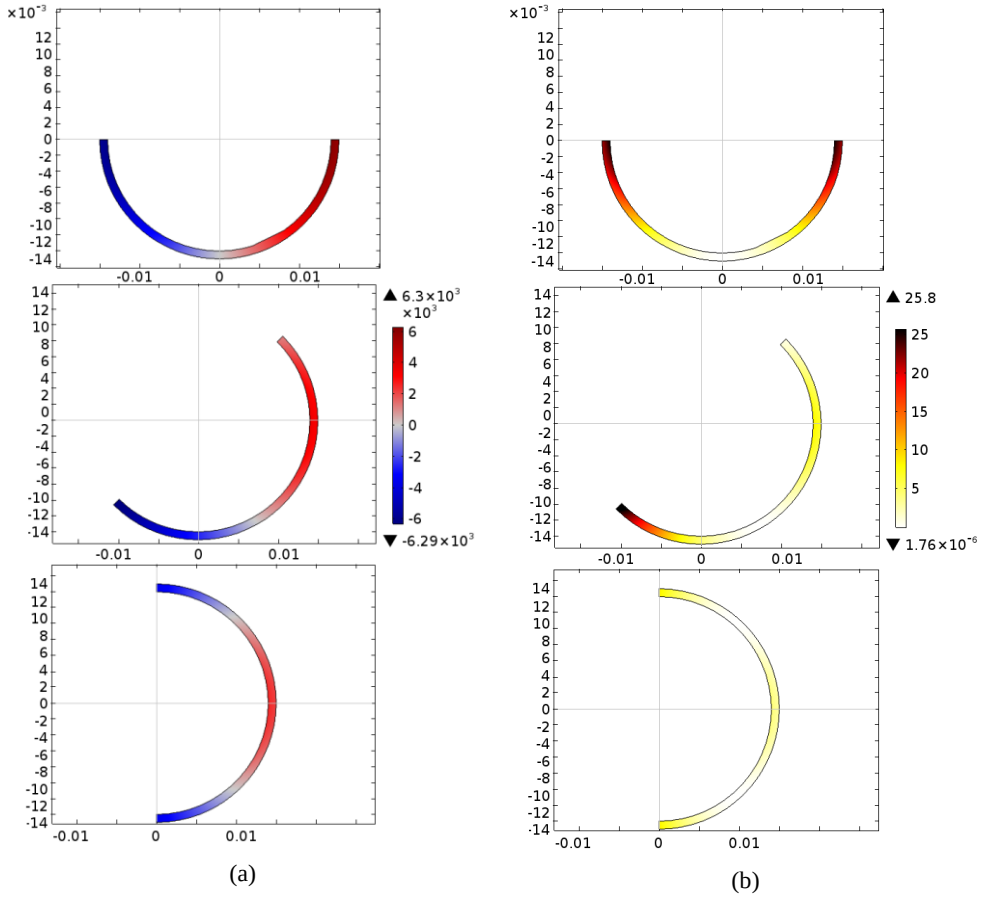

Fig. 4. Distribution of eddy currents density j in A/m^2: (a) and heat generation caused by them in W/m^3; (b) shown on the cross-section of the split shell with angle β of (top to bottom) 0°, 45°, 90°

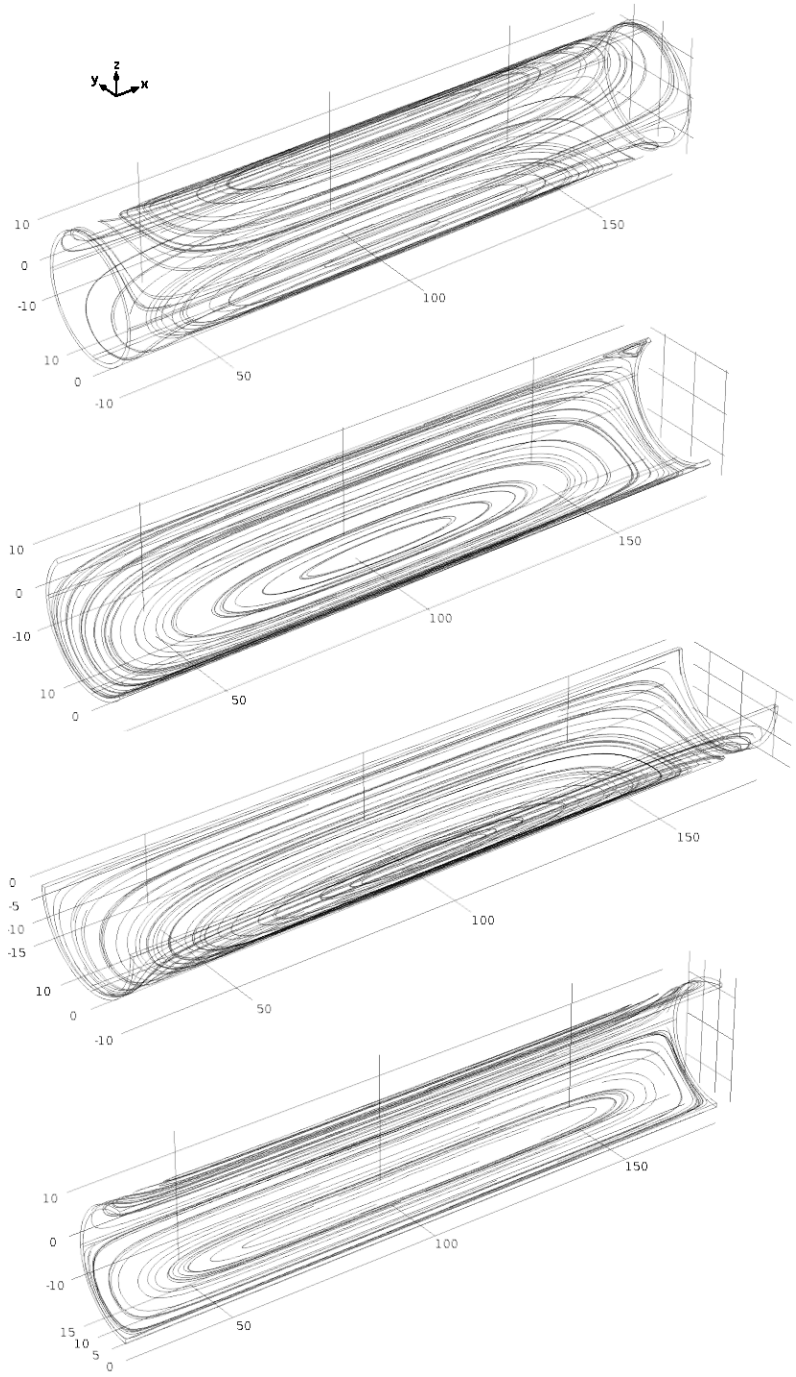

Fig. 5. Isometric view of streamlines of eddy currents for (top to bottom) full shell, split shell with angle β of 45°, 0°, 90°

cut along the line connecting the axes of bus-bars ($\beta = 0°$) the distribution of current and the total size of heat generation remain the same as in an undivided shell, as can be seen in Figures 4 and 5.The single loop which is observed is basically the half of current distribution in a full shell. Zero current and the highest heat generation also occur in the same respective regions.

When $\beta = 45°$ a single loop is still observed. However, it has a different shape. Location with zero current is displaced and the highest current is observed on the edge of the half of shell further from the intersection with the line connecting the axes of bus-bars. The distribution of currents and heat generation is not symmetrical. The current is more extensively distributed in the section of the shell close to the horizontal line. Total heat generation is approximately 41% lower than in the case of a full shell.

When the split of the shell is positioned perpendicularly to the line connecting the bus-bars ($\beta = 90°$) currents flow in two symmetrical loops separated in the central part of the half of the shell. Currents are strongest there and at the edges of the shell. Zero current is observed approximately at 22.5° from the horizontal line, halfway between the edges and the center of the half of the shell. Eddy currents are much weaker than in the case of the full shell and the total heat generation is approximately 79% lower. The difference decreases slightly with the increase of parameter ζ.

Figure 6 shows that the total eddy current heat generation occurring in a split shell decrease with the increase of angle β and the decrease of geometrical parameter ζ. The value is strongly dependent on angle β. For given ζ heat generation is between 4.82 and 4.63 times higher when β is 0° compared to value when β is 90°. The dependence of heat generation on ζ is weaker and decreases with the increase of β. For given β they are between 1.51 to 1.57 times higher when ζ is varied between 0.285 and 0.35. The highest value of the total heat generation in an analysed range is $9.78 \cdot 10^{-4}$ W/m, observed for $\zeta = 0.35$ and $\beta = 0°$. The lowest value is $1.34 \cdot 10^{-4}$ W/m, almost 7.3 times less than the maximum, occurring at the other side of the analysed range for $\zeta = 0.285$ and $\beta = 90°$.

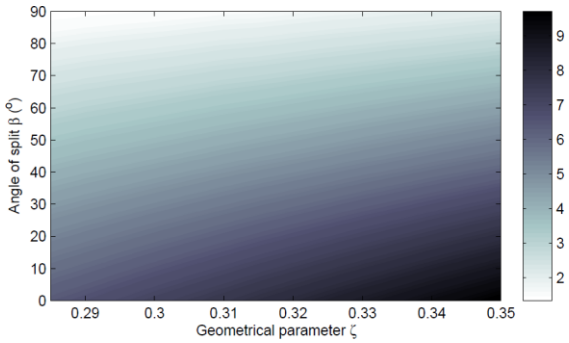

Fig. 6. Dependence of eddy current heat generation in W/m on ζ and angle β for split shell given in W/m based on 3D numerical model

The calculated eddy current heat generation occurring in the shell is very small when compared to other heat inputs to the cryogenic system. There are going to be 6 by-pass lines with

a length of approximately 45 m connecting sections of the SIS100 accelerator [2]. The total heat generation according to the worst case scenario of analytical calculations will be approximately 0.29 W. In the best case scenario heat generation will be much lower, approximately 0.036 W. Expected heat leaks to cryogenic transfer lines of the SIS-300 accelerator are at a level of 165 W, for SIS-100 they are expected to be slightly lower [13]. The total heat load at 4.5 K is 4289 W. Therefore, in optimal conditions, the contribution of heat load from eddy currents in the shell of bus-bar is almost negligible.

The application of a split tube and its proper placement allows to significantly reduce heat generation. From manufacturing point of view, the split is actually a more favourable option, as it allows for easier assembly. By placing it at a proper angle with respect to the position of bus-bars some savings of heat load can be obtained. As shown, the radial position of bus-bars inside the shell is less important and other issues, such as mechanical strength of separators, avoidance of cross-talks or the risk of discharge can be prioritised.

5. Conclusion

The amount of heat generated by eddy currents in the shell of a bus-bar was found to be in the range of 0.29-0.036 W. Both this values are small when related to other heat sources present in the accelerator system. From a manufacturing and thermal point of view it is better to apply a split shell. The generation of heat in a full shell is the same as in the worst case of a split shell. Amount of heat generated in the split shell is strongly affected by geometric conditions, especially by the angle between the split and bus-bar assembly. The optimal placement of split for which the heat generation is the smallest was found to be perpendicular to the line connecting the bus-bars.

Acknowledgements

This work has received funding from Ministry for Science and Higher Education under FAIR in-kind Contract between Facility for Antiproton and Ion Research in Europe GMbH, Jagiellonian University and Wroclaw University of Science and Technology.

References

[1] FAIR collaboration, *FAIR Baseline Technical Report*, March 2006, vol. 1 (2006).
[2] Eisel T., Chorowski M., Iluk A. et al., *Local Cryogenics for the SIS100 at FAIR*, IOP Conference Series: Materials Science and Engineering, vol. 101, no. May 2016, p. 012075 (2015).
[3] Acker D., Bleile A., Fischer E. et al., *Development of FAIR superconducting magnets and cryogenic system*, GSI Scientific Report, no. 506065, pp. 118-119 (2010).
[4] Khodzhibagiyan H., Drobin V., Fischer E. et al., *Design and study of new cables for superconducting accelerator magnets: Synchrotron SIS 100 at GSI and NICA collider at JINR*, Journal of Physics: Conference Series, vol. 234, p. 022017 (2010).
[5] Raach H., Schroeder C., Floch E. et al., *14 kA HTS current leads with one 4.8 K helium stream for the prototype test facility at GSI*, Physics Procedia, vol. 67, pp. 1098-1101 (2015).

[6] Xiang Y., Kauschke M., Schroeder C., Kollmus H., *Cryogenics for super-FRS at FAIR*, Physics Procedia, vol. 67, pp. 847-852 (2015).
[7] Kauschke M., Xiang Y., Schroeder C. et al., *Cryogenic Supply for Accelerators and Experiments at FAIR*, AIP Conference Proceedings, vol. 1200, no. 2014 (2014).
[8] Bleile A., Fischer E., Freisleben W. et al., *Thermodynamic properties of the superconducting dipole magnet of the SIS100 synchrotron*, Physics Procedia, vol. 67, pp. 781-784 (2015).
[9] Fischer E., Kurnyshov R., Shcherbakov P., *Analysis of coupled electromagnetic-thermal effects in superconducting accelerator magnets*, Journal of Physics: Conference Series, vol. 97, p. 012261 (2008).
[10] Stafiniak A., Floch E., Schroeder C. et al., *The GSI Cryogenic Prototype Test Facility – First Experience Gained on 2-Phase-Flow Superconducting Prototype Magnets of the FAIR Project*, IEEE Transactions on Applied Superconductivity, vol. 19, no. 3, pp. 1150-1153 (2009).
[11] Fischer E., Mierau A., Schnizer P. et al., *Thermodynamic Properties of Fast Ramped Superconducting Accelerator Magnets for the Fair Project*, AIP Conference Proceedings, vol. 552, no. 2004, pp. 989-996 (2010).
[12] Fischer E., Schnizer P., Mierau A. et al., *Status of the Superconducting Magnets for FAIR*, GSI Scientific Report, vol. 24, no. 3, pp. 474-475 (2014).
[13] Ageev A., Kozub S., Zintchenko S., Zubko V., *Cooling System of the SIS300 Accelerator Heat Load of SIS300 Cryogenic System*, Proceedings of RuPAC-2010, pp. 303-305 (2010).
[14] Fischer E., Schnizer P., Mierau A. et al., *Design and Test Status of the Fast Ramped Superconducting SIS100 Dipole Magnet for FAIR*, IEEE Transactions on Applied Superconductivity, vol. 21, no. 3, pp. 1844-1848 (2011).
[15] Bleile A., Fischer E., Khodzhibagiyan H. et al., *Investigation of the cooling conditions for the Fast Ramped Superconducting Magnets of the SIS100 Synchrotron*, Journal of Physics: Conference Series, vol. 507, no. 3, p. 032007 (2014).
[16] Rong J., Huang X., *AC Loss of ITER Feeder Busbar in 15MA Plasma Current Reference Scenario*, Journal of Fusion Energy, vol. 35, no. 2, pp. 173-179 (2016).
[17] Fischer E., Kurnyshov R., Shcherbakov P., *Analysis of the Eddy Current Relaxation Time Effects in the FAIR SIS 100 Main Magnets*, IEEE Transactions on Applied Superconductivity, vol. 17, no. 2, pp. 1173-1176 (2007).
[18] Stafiniak A., Szwangruber P., Freisleben W., Floch E., *Electrical integrity and its protection for reliable operation of superconducting machines*, Physics Procedia, vol. 67, pp. 1106-1111 (2015).
[19] Schnizer P., Mierau A., Bleile A. et al., *Low-temperature test capabilities for the superconducting magnets of FAIR*, IEEE Transactions on Applied Superconductivity, vol. 25, no. 3 (2015).
[20] Ho C., Chu T., *Electrical resistivity and thermal conductivity of nine selected AISI stainless steels*, Cindas Report 45 (1977).